Published in final edited form as:
Nanotoxicology. 2011 December ; 5(4): 592–605. doi:10.3109/17435390.2010.541292.

Pharmacotoxicology of monocyte-macrophage nanoformulated antiretroviral drug uptake and carriage

Rafael F. Bressani[1], **Ari S. Nowacek**[1], **Sangya Singh**[1], **Shantanu Balkundi**[1], **Barrett Rabinow**[2], **JoEllyn McMillan**[1], **Howard E. Gendelman**[1], and **Georgette D. Kanmogne**[1,*]

[1]Department of Pharmacology and Experimental Neuroscience, University of Nebraska Medical Center, Omaha, NE 68198-5215

[2]Baxter Healthcare Corporation, Round Lake, IL 60073

Abstract

Limitations inherent to antiretroviral therapy (ART) in its pharmacokinetic properties remain despite over 15 years of broad use. Our laboratory has pioneered a means to improve ART delivery through monocyte-macrophage carriage of nanoformulated drug-encapsulated particles (nanoART). To this end, our prior works sought to optimize nanoART size, structure, and physical properties for cell uptake and antiretroviral activities. To test the functional consequences of indinavir, ritonavir, and efavirenz formulations we investigated relationships between human monocyte and macrophage cytotoxicities and nanoART dose, size, surfactant, and preparation. Wet-milled particles were significantly more cytotoxic to monocytes-macrophages than those prepared by homogenization; with concurrent induction of tumor necrosis factor-alpha. Interestingly, pure suspensions of indinavir and ritonavir at 0.5mM, and efavirenz at 0.1mM and 0.5mM also proved cytotoxic. Individual surfactants and formulated fluconazole neither affected cell function or viability. Although nanoART did not alter brain tight junction proteins ZO-2 and occludin, 0.5mM ritonavir formulations did alter brain transendothelial electric resistance. These results underscore the importance of evaluating the physicochemical and functional properties of nanoART before human evaluations.

Keywords

nanoART; pharmacotoxicology; monocytes and macrophages; blood-brain barrier; antiretroviral therapy; nanomedicine; nanotoxicity

INTRODUCTION

Over 33 million individuals worldwide are infected with the human immunodeficiency virus (HIV) greatly impacting the social and economic infrastructures of resource limited areas (Beauliere et al., 2010; UNAIDS, 2009). In attempts to combat the ravages of this pandemic substantive efforts by governments and the international community are underway to make

*Corresponding author: Georgette D. Kanmogne, PhD, MPH, Department of Pharmacology and Experimental Neuroscience, University of Nebraska Medical Center, Omaha NE 68198-5215, Tel: 402-559-4084 Fax: 402-559-8922 gkanmogne@unmc.edu.

Authorship Contribution

RFB, SS, and ASN performed research; ASN, SB, JM, and BR prepared nanoART; HEG participated in the study design, assisted in data interpretation, and edited the manuscript; GDK designed and supervised the study, collected and analyzed the data, and wrote the paper.

Potential Conflicts of Interest

The authors declare that they have no competing interests

antiretroviral therapy (ART) widely available (Bartlett and Shao, 2009; Beauliere et al., 2010; Kim and Ammann, 2004). Unfortunately, limitations remain including a short ART half-life and pills, even when combined, need be administered several times/day and at regular intervals to maintain therapeutic blood levels (Darwich et al., 2008; Moreno et al., 2010). Moreover, failure to adhere to treatment regimens increases the risk of uncontrolled viral replication and mutations. Development of viral resistance, CD4+ T cell depletion, and disease progression is the common result (Conway, 2007; Kiertiburanakul and Sungkanuparph, 2009; Sandelowski et al., 2009; Waters and Nelson, 2007). Such events are further complicated by co-morbid conditions and illicit drug use (Berg et al., 2007; Conway, 2007; Sandelowski et al., 2009). We postulate that repackaging traditional antiretroviral medications into crystalline nanoparticles (nanoART) can improve both the pharmacokinetics and biodistribution of ART. This can be realized through increased drug dosing intervals thus effecting treatment compliance, and clinical outcomes (Nowacek and Gendelman, 2009). To this end, our prior works demonstrated the efficient cellular uptake, distribution, and release of nanoART in both *in vitro* and animal models of human disease (Beduneau et al., 2009; Dou et al., 2006; Dou et al., 2009; Dou et al., 2007; Nowacek et al., 2009b). This work demonstrated that monocyte-derived macrophages (MDM) that disseminate virus could also be harnessed to deliver nanoART to parallel tissue sites of active HIV-1 replication (Beduneau et al., 2009; Dou et al., 2006; Dou et al., 2009; Dou et al., 2007; Gorantla et al., 2006; Nowacek and Gendelman, 2009; Nowacek et al., 2009b). Despite these advances, what remained unanswered was the effect of nanoART cell loadings on cellular functions. To this end, we investigated the effect of nanoART carriage on monocyte and MDM viability and endothelial barrier functions.

MATERIALS AND METHODS

NanoART preparation and characterization

NanoART were manufactured from two HIV-1 proteases, indinavir and ritonavir (IDV and RTV) and one non-nucleoside reverse transcriptase inhibitor, efavirenz (EFV). The nanoparticles were manufactured by high-pressure homogenization and wet milling. When used for either homogenization or wet milling, IDV-sulfate was freebased using 1N NaOH solution to remove the sulfate group and generate pure drug. RTV and EFV did not have attached a sulfate group and thus were not subjected to freebasing. The surfactants used for nanoART included a block copolymer of ethylene oxide and propylene oxide (Poloxamer 188; P-188, Spectrum Chemicals, Gardena, CA), 1,2-distearoylphosphatidyl-ethanolamine-methyl-poly-ethylene-glycol (DSPE-mPEG2000) (Genzyme, Cambridge, MA), poly (lactic-co-glycolic acid) (PLGA) (Sigma-Aldrich, St. Louis, MO), and cetyltrimethyl ammonium bromide (CTAB, Sigma-Aldrich) (Table 1).

For homogenization, nanoART were prepared using an Avestin C5 high-pressure homogenizer (Nowacek et al., 2009b). The nanosized drug crystals were coated with individual surfactants at concentrations (weight/weight percent) consisting of P-188 (0.5%) and $mPEG_{2000}$-DSPE (0.2%). Nanosuspensions were formulated at a pH of 7.8 using either 10 mM sodium phosphate or 10 mM HEPES buffer. Tonicity was adjusted with glycerin (2.25%) or with sucrose (9.25%). Drug was added to the surfactant solution to make a concentration of approximately 2% [weight to volume ratio (%)]. Lissamine rhodamine B 1,2-dihexadecanoyl-sn-glycero-3-phosphoethanolamine, triethylammonium salt (rDHPE; Invitrogen, Carlsbad, CA) was used to label nanoART, which appeared as a red fluorescence. Each suspension was prepared by adding crystalline drug to a surfactant solution and mixing for 4 – 7 min using an Ultra-Turrax T-18 (IKA® Works Inc., Wilmington, NC) rotor-stator mixer to reduce initial particle size. The suspension was homogenized at 20,000 pounds per square inch for approximately 30 passes or until desired

particle size was reached. Nanoparticles of fluconazole, which was used as control drug, were manufactured using the same methods mentioned above (Table 1).

For wet milling, IDV and RTV were suspended in a buffer containing 10 mM HEPES, pH 7.8 and individual surfactant (0.5 % P188, 0.5 % SDS for IDV, and 0.3 % P188, 0.1 % $mPEG_{2000}$-DSPE for RTV). Sucrose (2.8%) was added to adjust the tonicity. As with homogenization, fluconazole controls were made in the same buffer using similar surfactant ratios (Table 1). Again, using a T-18 mixer each formulation was mixed to obtain a homogenous solution. The mixture was then transferred to a NETZSCH MicroSeries Wet Milling Chamber filled with 50 mL of 0.8 mm grinding media (Zirconium ceramic beads). The sample was run for 30 min to 1 hour (h) at speeds between [600-4320 rpm] in order to obtain desired particle size. The lipid based particles were comprised of the crystalline free-base drug coated and stabilized by phospholipids (Dou et al., 2007). Nanosuspension stability assays indicated stability of the suspensions for at least 1 month (data not shown).

To make EFV nanoparticles PLGA, CTAB, and EFV free base (12%, 1.0%, and 2.5%, respectively) were dissolved in dichloromethane and added to a 1% poly (vinyl) alcohol solution. Particle size was achieved by sonicating at 50% amplitude for 10 minutes using a 400/600-watt sonicator with 3/4-inch high gain probe. Particles were hardened by stirring overnight in order to evaporate dichloromethane. The suspension was centrifuged, washed with 18-MΩ water and decanted twice. The particles were suspended in 10% mannitol before being frozen or lyophilized for storage. For all nanosuspensions, particle size was measured by dynamic light scattering using a HORIBA LA 920 light scattering instrument (HORIBA Instruments Inc., Irvine, CA) (relative refractive index = 1.08 for IDV and 1.20 for RTV and EFV), and zeta potential was measured using a Brookhaven Zeta Plus potentiometer (Brookhaven Instruments Ltd., Chapel Hill, UK) by diluting 0.1 ml of the suspension into 9.9 ml of 10 mM HEPES, pH 7.4. The final drug content of all nanoART formulations was determined by reverse phase high performance liquid chromatography (RP-HPLC) as previously described (Nowacek et al., 2009b).

Scanning Electron Microscopy

Nanoformulations were vortexed for 20 sec in order to completely resuspend the particles. A small volume (10μl) of the suspension was transferred into a 1.5 ml micro-centrifuge tube containing 1 mL of 0.2 μm filtered distilled water. The diluted suspension was vortexed for 10 sec to ensure dispersion and a 50 μl aliquot of each nanoformulation was transferred to a Swinnex 13 Polypropylene filtration apparatus (Millipore, Billerica, MA) assembled with a Nuclepore Track-Etched 0.2 μm Polycarbonate filtration membrane (Whatman, Maidstone, UK). Prior to the addition of the diluted NP suspension the filtration apparatus was primed with 50 μl of 0.2 μm filtered distilled water. Vacuum was then applied to the apparatus until the entire volume had completely passed through the filtration membrane. Upon dryness, the membrane was affixed to an aluminum pin stub using double stick conductive carbon tape and sputter coated with palladium. The specimen stub was then imaged using a scanning electron microscope.

Human monocyte isolation and culture

Monocytes were obtained from HIV-1, HIV-2, and hepatitis B seronegative donor leukopaks, separated by countercurrent centrifugal elutriation and characterized as previously described (Gendelman et al., 1988; Kanmogne et al., 2007). Freshly elutriated monocytes were cultured for 7 days in Dulbecco's Modified Eagles Media containing 2 mM L-glutamine (Invitrogen), 10% heat-inactivated human serum, 100 μg/ml gentamicin, and 10μg/ml ciprofloxacin (Sigma) in the presence of 1,000 U/ml human recombinant macrophage colony stimulating factor (a generous gift from Wyeth Inc., Cambridge, MA).

NanoART uptake, retention, and release

MDM were treated with individual IDV, RTV, or EFV (0.1 to 0.5 mM) nanoformulations and each experimental condition was performed in triplicate. To assess nanoART uptake, cells were collected at 0.5, 1, 2, 4, 8, 12, and 24 hrs without media change and levels of drug in cell lysates quantified by RP-HPLC as previously described (Nowacek et al., 2009b; Rebiere et al., 2007; Weller et al., 2007). To evaluate the levels of drugs released into surrounding media by nanoART-treated cells, MDM were loaded with nanoART for 12 hrs, washed 3 times with PBS to remove any free drugs, and cultured for 15 days in drug free media with a half media exchange occurring every other day. On collection days, media and corresponding cells were collected and processed for measurement of drug content. All experiments were performed in triplicate and drug uptake, retention and release determined. For RP-HPLC analysis of drug concentration, triplicate 20-μl injections of each sample were run through a YMC Octyl C8 column (Waters Inc., Milford, MA) with a C8 guard cartridge using a Waters Breeze HPLC system with a Waters 2487 dual λ detector (Waters Inc., Milford, MA). Mobile phase consisting of 48% acetonitrile/52% of 25 mM KH_2PO_4, pH 4.15, was pumped at 0.4 ml/min with UV/Vis detection at 212 nm (Rebiere et al., 2007; Weller et al., 2007). For all nanoART formulations, the amounts of drug uptake, retention, and release were quantified using a standard curve of each free drug (0.025–100 μg/ml) prepared in methanol.

Cytotoxicity and measures of transendothelial electrical resistance (TEER)

Monocytes or MDM were cultured at cell concentrations of 6.25×10^5 cells/ml. These were treated with nanoformulations of IDV, RTV or EFV at 0.1 or 0.5 mM for 12 hrs at 37°C, 5% CO_2. Following loading of each nanoformulation, cells were washed with serum-free culture media to remove excess NP and cytotoxicity assessed over 48 hrs using alamarBlue™ assay (AbD Serotec, Raleigh, NC) according to the manufacturer's instructions.

Primary human brain microvascular endothelial cells (HBMEC) were isolated from the temporal cortex of brain tissue obtained during surgical removal of epileptogenic cerebral cortex in adult patients and cultured as we previously described (Chaudhuri et al., 2008; Kanmogne et al., 2007). For TEER measurements, HBMEC were seeded on gold-film electrode surface and cultured to confluence. Monocytes and MDM were loaded with nanoART for 12 hrs as described above, washed, and cultured for 24 hrs (37°C, 5% CO_2). Confluent HBMEC were exposed to nanoART-loaded cells or conditioned media (CM) from nanoART-loaded immunocytes, and TEER live-recorded readings were made before and after exposures.

Western blot assays

Monocytes were loaded with IDV or RTV nanoformulations as described above and then washed to remove non-phagocytized drugs. Controls and nanoART-loaded monocytes were then co-cultured for 2 hrs with HBMEC, and HBMEC were washed three times with phosphate buffered saline (PBS) to remove monocytes. Cell lysates were then prepared from HBMEC and protein quantitation and Western blot assays performed as described previously (Kanmogne et al., 2005; Kanmogne et al., 2007). ZO-2, occludin and actin antibodies were purchased from Invitrogen.

Tumor necrosis factor alpha and interleukin-12 (TNF-α and IL-12) immunoassays

Monocytes and macrophages were loaded for 12 hrs with nanoART as described then washed to remove excess NP, resuspended in fresh media and cultured for 24 hrs. Following culture, supernatant was collected, and TNF-α and IL-12 p70 quantified by bead-based immunoassay using human TNF-α and IL-12p70 Flex Sets (BD Biosciences, San Jose, CA),

according to the manufacturer instructions. To determine the potential effect of secreted factors from nanoART-loaded cells on the blood-brain barrier (BBB), HBMEC were exposed for 24 hrs to CM from controls and nanoART-loaded monocytes and macrophages. Media from HBMEC was collected, and TNF-α and IL-12p70 quantified as described above. All cytokine results were independently confirmed by cytokine ELISA using ELISA kits from eBioscience (San Diego, CA).

RESULTS

Manufacture and characterization of nanoART

NanoART, prepared from free-base drug, were manufactured as nanosized drug crystals coated with phospholipid surfactants (IDV and RTV) or drug dissolved in a PLGA copolymer solution (EFV). The overall physical properties of the nanosuspensions were similar in charge (Table 1) but varied greatly in size and shape (Fig. 1, Table 1). The largest particle size was 1600 nm (H1008) while the smallest was 204 nm (H2009). The charges of all particles were negative (≤ -18 mV) except for P4033, which was positive (+7.4 mV). Nanoformulations manufactured by homogenization had smooth edges, with boulders-like shapes (IDV) or short rod-shapes (Fig. 1). NanoART manufactured by wet milling had rough edges and sharper corners, with ellipsoid shapes (IDV) or short rod-shapes (RTV) (Fig. 1).

NanoART uptake, drug retention and release

To quantify IDV, RTV, and EFV uptake, cellular contents of drugs were analyzed by RP-HPLC (Nowacek et al., 2009b). NanoART uptake was rapid and drug levels plateaued at 12 hrs. H1013a and H1013b showed the highest levels of IDV uptake, retention and release (Fig. 2). At all time points, H1008 uptake was 5 to 8-fold lower than H1013a or H1013b uptake ($P<0.001$). The low H1008 uptake correlated with its non-retention in cells and very low levels present in the surrounding media. H1008 retention and release was 16- to 700-fold lower than H1013a and H1013b retention and release ($P<0.001$) (Fig. 2). Overall, H1013a and H1013b showed similar patterns of cellular uptake, retention and release. Similar to H1008, wet milled IDV (M1002) also exhibited poor uptake, low release and very low retention. Compared to the homogenized H1013a and H1013b formulations, uptake of M1002 was 2.7- to 7-fold lower, ($P<0.001$); M1002 release from day-1 to day-9 was 2.6- to 56-fold lower ($P<0.001$), with no M1002 present in surrounding media after day-9; M1002 cellular retention was 32- to 60-fold lower than H1013a or H1013b retention ($P<0.001$).

The highest levels of RTV uptake, retention, and release were observed with H2014 and H2013 (Fig. 2). Compared to H2014 and H2013, H2009 uptake was 4- to 10-fold lower between 0.5 to 4 hrs, and 1.6- to 2.4-fold lower between 8 and 24 hrs ($P<0.001$). H2009 release between day 3 and day 11 was 1.2- to 11-fold lower ($P<0.001$), while H2009 retention was 2- to 4.8-fold lower ($P<0.001$), with almost no H2009 detected in cells or media after day-11 (Fig. 2). Compared to H2014 and H2013 (both homogenized RTV), uptake of milled RTV (M2006) was 1.2- to 2.4-fold lower, M2006 retention was 1.2- to 4.3-fold lower, while there was no significant difference in the levels of H2014, H2013, and M2006 released into the surrounding media (Fig. 2). The cellular uptake, retention, and release of M2006 were higher than those of H2009. P4033 showed the lowest levels of uptake, retention and release. Maximal P4033 uptake was 8- to 33-fold lower than maximal IDV uptake, and 15- to 25-fold lower than maximal RTV uptake (Fig. 2).

Cytotoxicity profiles of nanoART in human monocytes and MDM

We evaluated the toxicity of nine independent nanoART formulations manufactured by three different methods: homogenization, wet milling, and sonication. These included six

homogenized (three each for IDV and RTV), two wet-milled (one IDV and one RTV), and one sonicated (EFV) nanoART (Table 1). For control, we used similar concentrations of free IDV, RTV, or EFV without surfactant, and similar amounts of each surfactant without ART drugs (fluconazole was used to make surfactant coated control nanoparticles). Viability and functional tests were performed on human monocytes and MDM; for each nanoART, two different concentrations were investigated (0.1 mM and 0.5 mM) based on prior laboratory studies (Dou et al., 2006; Dou et al., 2009; Dou et al., 2007; Nowacek et al., 2009b), with the exception of H2009 that was investigated at 0.18 mM and 0.27 mM, based on prior toxicity profile studies. Evaluation of toxicity over 48 hrs by alamarBlue™ redox assay showed that at 0.1 mM concentration, homogenized IDV and RTV nanoformulations induced only modest reductions (7 to 21%) in monocyte and MDM viability. Free IDV and RTV (without NP) did not induce any cell toxicity at 0.1 mM but free EFV decreased monocyte viability by up to 32% while nanoformulated EFV only decreased cell viability by 9 to 12% at 0.1 mM (Fig. 3). Toxicity increased with higher drug concentrations (0.5 mM), with increased cytotoxicity observed in cells exposed to free RTV or EFV when compared to cells exposed to nanoformulated drugs. At 0.5 mM, free RTV decreased monocyte viability by 26 to 62% while H2014 and H2013 decreased cell viability by 12 to 33% and 14 to 44% respectively. Similarly, free RTV decreased MDM viability by up to 61%, while H2014 and H2013 decreased cell viability by 17 to 44% (Fig. 3). At both lower and higher concentrations, H2009 decreased monocyte and MDM viability by 8 to 26% and 22.7 to 37% respectively (Fig. 4). Overall, these results demonstrate that the degree of nanoART cytotoxicity is both formulation and drug concentration dependent.

Comparison of nanoformulated drugs prepared by homogenization and wet milling showed that wet milled M1002 and M2006 induced significantly more toxicity in monocytes and MDM than similar homogenized formulations. Homogenized IDV or RTV at 0.1 mM induced little or no toxicity in monocytes and MDM (Fig. 3 and 5), while similar concentrations of M1002 decreased monocyte and MDM viability by 6 to 22% and 7 to 10% respectively (Fig. 5); 0.1 mM M2006 decreased monocyte and MDM viability by 18 to 20% and 18 to 53% respectively (Fig. 5). Higher concentrations (0.5 mM) of H1008 and H2014 decreased monocyte and MDM viability by a maximum of 23 and 33% while M1002 decreased monocyte and MDM viability by up to 69% and M2006 decreased monocyte and MDM viability by up to 59% ($P<0.001$, Fig. 5). Additional control experiments were performed to determine the effects of surfactants alone on cell viability. These surfactants were prepared by homogenization and wet milling using fluconazole (Table 1), and additional controls include fluconazole without surfactant. All surfactants and fluconazole controls showed limited or no toxicity in monocytes and MDM (Fig. 6).

NanoART affects brain endothelial and barrier functions

We performed experiments to determine whether monocytes and MDM loaded with nanoART (H1008, H1013b, H2014 and H2013) or factors secreted by these nanoART-loaded monocytes and MDM can alter endothelial barrier properties and function. For this purpose, we exposed HBMEC to monocytes and MDM carrying nanoART or to CM from nanoART-loaded monocytes and MDM, and we assessed their effects on TEER. Exposure of HBMEC to monocytes or MDM loaded with 0.1 mM nanoART, or CM from monocytes or MDM loaded with 0.1 mM nanoART did not alter TEER (data not shown). Exposure of HBMEC to monocytes loaded with 0.5 mM nanoART or CM from monocytes loaded with 0.5 mM nanoART also did not alter TEER (Fig. 7A-D) nor did exposure of HBMEC to MDM loaded with 0.5 mM nanoART (Fig. 7E,F). Exposure of HBMEC to CM from MDM loaded with 0.5 mM H1008 decreased TEER by 5%, but this decrease was not statistically significant. However, CM from MDM loaded with 0.5 mM nanoformulated RTV decreased TEER by 12% (Fig. 7G,H, $P<0.01$).

To further determine the effect of monocytes and macrophages carrying NP on BBB integrity, we evaluated the expression of tight junction proteins ZO-2 and occludin on HBMEC co-cultured with monocytes loaded with H1008, H1013b, H2014 or H2013. Compared to control HBMEC not exposed to monocytes, or HBMEC exposed to monocytes without nanoART, nanoART loading did not alter ZO-2 and occludin expression in HBMEC (Fig. 8A).

NanoART affects cell-associated TNF-α and IL-12 expression

In a first series of experiments to determine whether nanoART alter cytokine secretion in immunocytes and brain endothelial cells, we used a cytometric bead array with human TNF-α and IL-12p70 Flex sets to quantify the levels of TNF-α and IL-12p70 in controls, monocytes and MDM exposed to nanoformulations of IDV, RTV and EFV. To further determine whether nanoART or any NP-induced factor may alter the BBB immune response, we measured the levels of TNF-α and IL-12p70 in primary HBMEC exposed to CM from monocytes and MDM loaded with nanoformulations of IDV, RTV and EFV, as well as HBMEC exposed to CM from control monocytes and MDM (not exposed to NP or exposed to surfactants only). None of the six homogenized nanoART induced TNF-α or IL-12p70 secretion in monocytes but milled formulations induced a moderate increase in cytokine levels. Compared to homogenized nanoART and controls, M1002 increased TNF-α levels in monocytes by 3- to 7.6-fold (Fig. 8B) and M2006 increased TNF-α levels by 3- to 4-fold (Fig.8C). None of the nanoART or free drugs induced TNF-α or IL-12p70 expression in MDM or HBMEC (data not shown).

DISCUSSION

Cell-based carriage utilizes monocytes-macrophages for nanoART uptake, carriage and drug release to sites of active viral replication. Nanoparticles cytoxicities were measured in this report to ensure that this drug delivery system itself does not affect disease. We hypothesized that the physical, biochemical and biological properties of nanoART such as particle shape, size, concentration, surfactant, drug, and manufacturing method could affect monocyte-macrophage cytotoxicity profiles. With this in mind, nanoformulated IDV, RTV, and EFV prepared by homogenization and wet milling were examined for their effects on cellular viability and function. Using primary HBMEC, we assessed the effect of nanoART on barrier function to determine whether these nanoformulations could alter the BBB integrity. The toxicity of the nanoformulations varied between monocytes and macrophages, drug, formulation, and manufacturing methods. The mechanism underlining the differential toxicities is not known, but it is possible that with large size (1600 nm) and poor uptake, H1008 did not aggregate on the cell's surface. On the contrary, due to their much smaller sizes more H2009 and EFV could be retained on the cell surface affecting the integrity of the cell membrane. In fact, our data demonstrate that the amounts of H1008 in cells or culture media from one to 15 days after nanoART loading was less than 1.6 μg /ml, while the amounts of H2009 from day-1 to day-15 varied from a maximum of 23 to 8.7 μg /ml, and that of P4033 varied from a maximum of 8 to 1.7 μg/ml (Fig. 2).

Particle charge could have contributed to EFV toxicities. EFV was the only formulation with a positive zeta potential (+7.4). The zeta potential is the overall charge a particle acquires in a specific medium and its magnitude provides an indication of the particle stability. It has been shown that particles with low (positive or negative) zeta potentials do not disperse well and are more unstable (Dougherty et al., 2008; Ghosh et al., 2008). The low positive zeta potential of P4033 could also have decreased its stability, and increased aggregation could also have contributed to the low cellular uptake. NanoART manufacturing also influenced the outcomes seen. Indeed, wet-milled formulations of both IDV and RTV showed reduced uptake, increased toxicity in both monocytes and MDM and increased TNF-α expression in

monocytes, compared to similar formulations prepared by homogenization. The increased toxicity of M1002 versus H1008 could be due to the presence of SDS in the surfactant of the milled nanoparticles in contrast to Tween 80 in the homogenized particles. The surfactant combination of P188 and SDS alone does not appear to be toxic as evidenced by the lack of toxicity of M5004. However, the combination of surfactant and drug could result in differences in toxicological characteristics of the particles.

Wet milling produces small particles by fractionating the surfactant-coated drug crystals down to smaller sizes, and the shape of the particles is determined by the shape of the fractionated crystals. Homogenization produces particles by passing the surfactant-coated crystals through a narrow bore under high pressure. Thus the particles produced by homogenization have smoother edges and are more uniform in shape than those produced by wet milling (Fig. 1). Particle shape affects MDM uptake, retention, and nanoART antiretroviral efficacy (Nowacek et al., in submission); the variation in particle shape could affect the methods and mechanisms of cellular uptake, and particles trafficking inside the cells, resulting in variations in toxicity. Other studies have reported that the biological effects of nanomaterials can be greatly influenced by the mechanisms of internalization, trafficking and sub-cellular storage. (Slowing et al., 2006; Vallhov et al., 2007). Studies are currently under way in our laboratories to determine how nanoART are taken up, trafficked, and stored by MDM, and how these may ultimately affect their function. The increased toxicity of milled nanoART over homogenized nanoART suggests that the properties of milled nanoART may adversely affect cell viability and increase the risk of inflammation, compared to homogenized formulations.

Although nanomedicine is a rapidly growing discipline with great potentials in pharmaceutics and pharmacology research where its explicit purpose is to improve drug delivery and pharmacokinetics its perils are also appreciated (Debbage, 2009; Gendelman et al., 2008; Khemtong et al., 2009). Targeted delivery of therapeutically beneficial compounds such as ART serves to combat viral infections even within their hard-to-treat tissue sanctuaries (Muthu and Singh, 2009). Specifically for HIV, nanoART has a number of distinct advantages over conventional ART. This includes reduction in dosing intervals and improved drug entry into viral tissue reservoirs including those housed within the central nervous system (CNS) (Nowacek and Gendelman, 2009; Nowacek et al., 2009a). Our previous reports demonstrated the synthesis, characterization, and tissue distribution of nanoART and showed that such nanoformulations can be loaded in MDM and delivered to viral sanctuaries (Dou et al., 2006; Dou et al., 2009; Dou et al., 2007; Nowacek et al., 2009b). These studies also showed significant increases in nanoART half-lives and anti-viral effects, compared to non-formulated (free) ART drugs (Dou et al., 2007; Nowacek et al., 2009b). Nonetheless, such new applications pose concerns in regards to toxicities of nanoformulated drugs on carrier cells and their effects on tissue viability and function. In the current study, attempts were made to address these concerns. Indeed, we demonstrate formulation and drug concentration dependent nanoART uptake, retention, release and toxicities.

We observed that the adverse effects of the nanoformulations were more pronounced in monocytes than MDM, with the exception of H2009. These findings are important and will guide subsequent studies to develop injectable nanoART for *in vivo* use. In fact, when drugs are administered by the intravenous (IV) route, they come into direct contact with blood monocytes within minutes and higher nanoART toxicities in monocytes suggest that IV injection may not be the appropriate administration route. We suspect that with other administration routes such as intradermal injections, monocyte uptake will be minimal and drug uptake will be mostly by macrophages or immature dendritic cells. Our subsequent studies will determine the optimal-safer method of nanoART administration *in vivo*. Drug

toxicity is a major issue for HIV-infected individuals on ART; this often causes patients to stop treatment, resulting in ART failure and emergence of drug-resistant viral strains that perpetuates the HIV/AIDS pandemic (Conway, 2007; Kiertiburanakul and Sungkanuparph, 2009; Sandelowski et al., 2009; Waters and Nelson, 2007). Controls used in this study included free IDV, RTV, and EFV (not mixed to surfactants), individual and combination surfactants without ART drugs, and fluconazole, an anti-fungal drug. The fact that these various controls induced very little or no cell toxicities suggests that formulation cytotoxicities were primarily due to nanoART drug composition, pharmacokinetics, and pharmacodynamics, not to the surfactants alone.

Prior reports demonstrated that nanoformulations of atazanavir, stavudine, delavirdine, and saquinavir increase drug concentration in HBMEC and alter BBB permeability (Chattopadhyay et al., 2008; Kuo and Su, 2007). Parallel studies showed that exposure of aluminum oxide NP to brain endothelial cells induced endothelial injury, loss of the tight junction protein claudin-5 and loss of mitochondrial membrane potential, with toxicities observed at 10 mM NP concentration (Chen et al., 2008). Our study of nanoART effects on the BBB showed that monocytes or MDM carrying four different nanoformulations of IDV and RTV did not induce significant alteration in the expression of tight junction proteins ZO-2 and occludin in HBMEC at 0.1mM and did not substantively alter TEER at both 0.1 and 0.5mM, although media from MDM carrying H2014 induced some decrease in brain TEER. Overall, direct toxicity of nanoART on cells was more pronounced than their effect on TEER and tight junction protein expression, which could be due to the fact that cytotoxicity and TEER measure different parameters. The alamarBlue™ is an oxidation-reduction (REDOX) assay that detects mitochondrial metabolic activity in cells and as such measures cell proliferation and/or cytotoxicity. These results suggest that nanoART toxicity in monocytes and MDM could be related to oxidative stress. In fact, there is evidence that clinically relevant concentrations of free EFV (3.2 to 12.7 μM) inhibit mitochondrial function in a concentration-dependent manner, and this was associated with reduced adenosine triphosphate levels and increased production of reactive oxygen species (Blas-Garcia et al., 2010). Interestingly, for many formulations, our study showed higher toxicities of free IDV, RTV, and EFV, compared to similar concentrations of nanoformulated IDV, RTV, and EFV. This suggests that nanomedicine-based delivery of ART drugs could diminish drug cytotoxicity.

TEER measures the endothelial barrier function (the resistance of the paracellular pathway between cells of the brain microvasculature), and any alteration in TEER likely occurs downstream, following physical alterations of the HBMEC and long after any change in mitochondrial or metabolic activity had occurred. Decrease in TEER was observed in HBMEC exposed to medium from H2014-loaded MDM. Our subsequent studies will determine whether this decrease in TEER is due to NP, reactive oxygen species or other soluble factors secreted by nanoART-loaded MDM. If the decreases in TEER are due to soluble factors, it is unlikely to be TNF-α or IL-12 because none of the ART nanoformulation induced TNF-α or IL-12p70 expression in MDM. Overall, the adverse toxicities were seen principally with high doses maximized in *in vitro* systems. Our study underscores the need to optimize individual formulations to correlate cytotoxicities with nanoART pharmacokinetics and pharmacodynamics to help ensure optimal therapeutic benefits. How the data is used to design human trials will be carefully developed as rodent then monkey pharmacokinetic examinations are undertaken.

Acknowledgments

We thank Dr. Han Chen and Dr. You Zhou of the University of Nebraska-Lincoln electron microscopy core facility for assistance with the SEM analysis. This work was supported by NIH grants RO1MH081780 (to GDK),

1P01DA028555-01, P01 NS043985 and P20 RR15635 (to HEG and GDK), 2R37 NS36126, PO1 NS31492, 2R01 NS034239, and P01MH64570 (to HEG).

References

Bartlett JA, Shao JF. Successes, challenges, and limitations of current antiretroviral therapy in low-income and middle-income countries. Lancet Infect Dis. 2009; 9:637–649. [PubMed: 19778766]

Beauliere A, Le Maux A, Trehin C, Perez F. Access to antiretroviral treatment in developing countries: Which financing strategies are possible? Rev Epidemiol Sante Publique. 2010; 58:171–179. [PubMed: 20430553]

Beduneau A, Ma Z, Grotepas CB, Kabanov A, Rabinow BE, Gong N, Mosley RL, Dou H, Boska MD, Gendelman HE. Facilitated monocyte-macrophage uptake and tissue distribution of superparmagnetic iron-oxide nanoparticles. PLoS One. 2009; 4:e4343. [PubMed: 19183814]

Berg CJ, Michelson SE, Safren SA. Behavioral aspects of HIV care: adherence, depression, substance use, and HIV-transmission behaviors. Infect Dis Clin North Am. 2007; 21:181–200. x. [PubMed: 17502235]

Blas-Garcia A, Apostolova N, Ballesteros D, Monleon D, Morales JM, Rocha M, Victor VM, Esplugues JV. Inhibition of mitochondrial function by efavirenz increases lipid content in hepatic cells. Hepatology. 2010; 52:115–125. [PubMed: 20564379]

Chattopadhyay N, Zastre J, Wong HL, Wu XY, Bendayan R. Solid lipid nanoparticles enhance the delivery of the HIV protease inhibitor, atazanavir, by a human brain endothelial cell line. Pharm Res. 2008; 25:2262–2271. [PubMed: 18516666]

Chaudhuri A, Yang B, Gendelman HE, Persidsky Y, Kanmogne GD. STAT1 signaling modulates HIV-1-induced inflammatory responses and leukocyte transmigration across the blood-brain barrier. Blood. 2008; 111:2062–2072. [PubMed: 18003888]

Chen L, Yokel RA, Hennig B, Toborek M. Manufactured aluminum oxide nanoparticles decrease expression of tight junction proteins in brain vasculature. J Neuroimmune Pharmacol. 2008; 3:286–295. [PubMed: 18830698]

Conway B. The role of adherence to antiretroviral therapy in the management of HIV infection. J Acquir Immune Defic Syndr. 2007; 45(Suppl 1):S14–18. [PubMed: 17525686]

Darwich L, Esteve A, Ruiz L, Bellido R, Clotet B, Martinez-Picado J. Variability in the plasma concentration of efavirenz and nevirapine is associated with genotypic resistance after treatment interruption. Antivir Ther. 2008; 13:945–951. [PubMed: 19043929]

Debbage P. Targeted drugs and nanomedicine: present and future. Curr Pharm Des. 2009; 15:153–172. [PubMed: 19149610]

Dou H, Destache CJ, Morehead JR, Mosley RL, Boska MD, Kingsley J, Gorantla S, Poluektova L, Nelson JA, Chaubal M, Werling J, Kipp J, Rabinow BE, Gendelman HE. Development of a macrophage-based nanoparticle platform for antiretroviral drug delivery. Blood. 2006; 108:2827–2835. [PubMed: 16809617]

Dou H, Grotepas CB, McMillan JM, Destache CJ, Chaubal M, Werling J, Kipp J, Rabinow B, Gendelman HE. Macrophage delivery of nanoformulated antiretroviral drug to the brain in a murine model of neuroAIDS. J Immunol. 2009; 183:661–669. [PubMed: 19535632]

Dou H, Morehead J, Destache CJ, Kingsley JD, Shlyakhtenko L, Zhou Y, Chaubal M, Werling J, Kipp J, Rabinow BE, Gendelman HE. Laboratory investigations for the morphologic, pharmacokinetic, and anti-retroviral properties of indinavir nanoparticles in human monocyte-derived macrophages. Virology. 2007; 358:148–158. [PubMed: 16997345]

Dougherty GM, Rose KA, Tok JB, Pannu SS, Chuang FY, Sha MY, Chakarova G, Penn SG. The zeta potential of surface-functionalized metallic nanorod particles in aqueous solution. Electrophoresis. 2008; 29:1131–1139. [PubMed: 18246574]

Gendelman HE, Kabanov A, Linder J. The promise and perils of CNS drug delivery: a video debate. J Neuroimmune Pharmacol. 2008; 3:58. [PubMed: 18322803]

Gendelman HE, Orenstein JM, Martin MA, Ferrua C, Mitra R, Phipps T, Wahl LA, Lane HC, Fauci AS, Burke DS, et al. Efficient isolation and propagation of human immunodeficiency virus on recombinant colony-stimulating factor 1-treated monocytes. J Exp Med. 1988; 167:1428–1441. [PubMed: 3258626]

Ghosh S, Mashayekhi H, Pan B, Bhowmik P, Xing B. Colloidal behavior of aluminum oxide nanoparticles as affected by pH and natural organic matter. Langmuir. 2008; 24:12385–12391. [PubMed: 18823134]

Gorantla S, Dou H, Boska M, Destache CJ, Nelson J, Poluektova L, Rabinow BE, Gendelman HE, Mosley RL. Quantitative magnetic resonance and SPECT imaging for macrophage tissue migration and nanoformulated drug delivery. J Leukoc Biol. 2006; 80:1165–1174. [PubMed: 16908517]

Kanmogne GD, Primeaux C, Grammas P. HIV-1 gp120 proteins alter tight junction protein expression and brain endothelial cell permeability: implications for the pathogenesis of HIV-associated dementia. J Neuropathol Exp Neurol. 2005; 64:498–505. [PubMed: 15977641]

Kanmogne GD, Schall K, Leibhart J, Knipe B, Gendelman HE, Persidsky Y. HIV-1 gp120 compromises blood-brain barrier integrity and enhances monocyte migration across blood-brain barrier: implication for viral neuropathogenesis. J Cereb Blood Flow Metab. 2007; 27:123–134. [PubMed: 16685256]

Khemtong C, Kessinger CW, Gao J. Polymeric nanomedicine for cancer MR imaging and drug delivery. Chem Commun (Camb). 2009:3497–3510. [PubMed: 19521593]

Kiertiburanakul S, Sungkanuparph S. Emerging of HIV drug resistance: epidemiology, diagnosis, treatment and prevention. Curr HIV Res. 2009; 7:273–278. [PubMed: 19442122]

Kim JY, Ammann A. Is the “3 by 5” initiative the best approach to tackling the HIV pandemic? PLoS Med. 2004; 1:e37. [PubMed: 15578107]

Kuo YC, Su FL. Transport of stavudine, delavirdine, and saquinavir across the blood-brain barrier by polybutylcyanoacrylate, methylmethacrylate-sulfopropylmethacrylate, and solid lipid nanoparticles. Int J Pharm. 2007; 340:143–152. [PubMed: 17418986]

Moreno S, Lopez Aldeguer J, Arribas JR, Domingo P, Iribarren JA, Ribera E, Rivero A, Pulido F. The future of antiretroviral therapy: challenges and needs. J Antimicrob Chemother. 2010; 65:827–835. [PubMed: 20228080]

Muthu MS, Singh S. Targeted nanomedicines: effective treatment modalities for cancer, AIDS and brain disorders. Nanomed. 2009; 4:105–118.

Nowacek A, Gendelman HE. NanoART, neuroAIDS and CNS drug delivery. Nanomedicine (Lond). 2009; 4:557–574. [PubMed: 19572821]

Nowacek A, Kosloski LM, Gendelman HE. Neurodegenerative disorders and nanoformulated drug development. Nanomedicine (Lond). 2009a; 4:541–555. [PubMed: 19572820]

Nowacek AS, Miller RL, McMillan J, Kanmogne G, Kanmogne M, Mosley RL, Ma Z, Graham S, Chaubal M, Werling J, Rabinow B, Dou H, Gendelman HE. NanoART synthesis, characterization, uptake, release and toxicology for human monocyte-macrophage drug delivery. Nanomedicine (Lond). 2009b; 4:903–917. [PubMed: 19958227]

Rebiere H, Mazel B, Civade C, Bonnet PA. Determination of 19 antiretroviral agents in pharmaceuticals or suspected products with two methods using high-performance liquid chromatography. J Chromatogr B Analyt Technol Biomed Life Sci. 2007; 850:376–383.

Sandelowski M, Voils CI, Chang Y, Lee EJ. A systematic review comparing antiretroviral adherence descriptive and intervention studies conducted in the USA. AIDS Care. 2009; 21:953–966. [PubMed: 20024751]

Slowing I, Trewyn BG, Lin VS. Effect of surface functionalization of MCM-41-type mesoporous silica nanoparticles on the endocytosis by human cancer cells. J Am Chem Soc. 2006; 128:14792–14793. [PubMed: 17105274]

UNAIDS. AIDS epidemic update. 2009 UNAIDS/09.36E / JC1700E.

Vallhov H, Gabrielsson S, Stromme M, Scheynius A, Garcia-Bennett AE. Mesoporous silica particles induce size dependent effects on human dendritic cells. Nano Lett. 2007; 7:3576–3582. [PubMed: 17975942]

Waters L, Nelson M. Why do patients fail HIV therapy? Int J Clin Pract. 2007; 61:983–990. [PubMed: 17504360]

Weller DR, Brundage RC, Balfour HH Jr, Vezina HE. An isocratic liquid chromatography method for determining HIV non-nucleoside reverse transcriptase inhibitor and protease inhibitor

concentrations in human plasma. J Chromatogr B Analyt Technol Biomed Life Sci. 2007; 848:369–373.

ABBREVIATIONS

ART	antiretroviral therapy
BBB	blood-brain barrier
CM	conditioned media
CNS	central nervous system
CTAB	cetyltrimethyl ammonium bromide
DSPE-mPEG2000	1,2-distearoylphosphatidyl-ethanolamine-methyl-poly-ethylene-glycol
EFV	efavirenz
HBMEC	human brain microvascular endothelial cells
HIV	human immunodeficiency virus
IDV	indivavir
IL	interleukin
MDM	monocyte-derived macrophages
MP	mononuclear phagocytes
NanoART	nanoformulated ART
NP	nanoparticles
P-188	poloxamer 188
PBS	phosphate buffered saline
PLGA	poly(lactic-co-glycolic acid)
REDOX	oxidation-reduction
RP-HPLC	reverse phase high performance liquid chromatography
RTV	ritonavir
TEER	transendothelial electric resistance
TNF-α	tumor necrosis factor-alpha

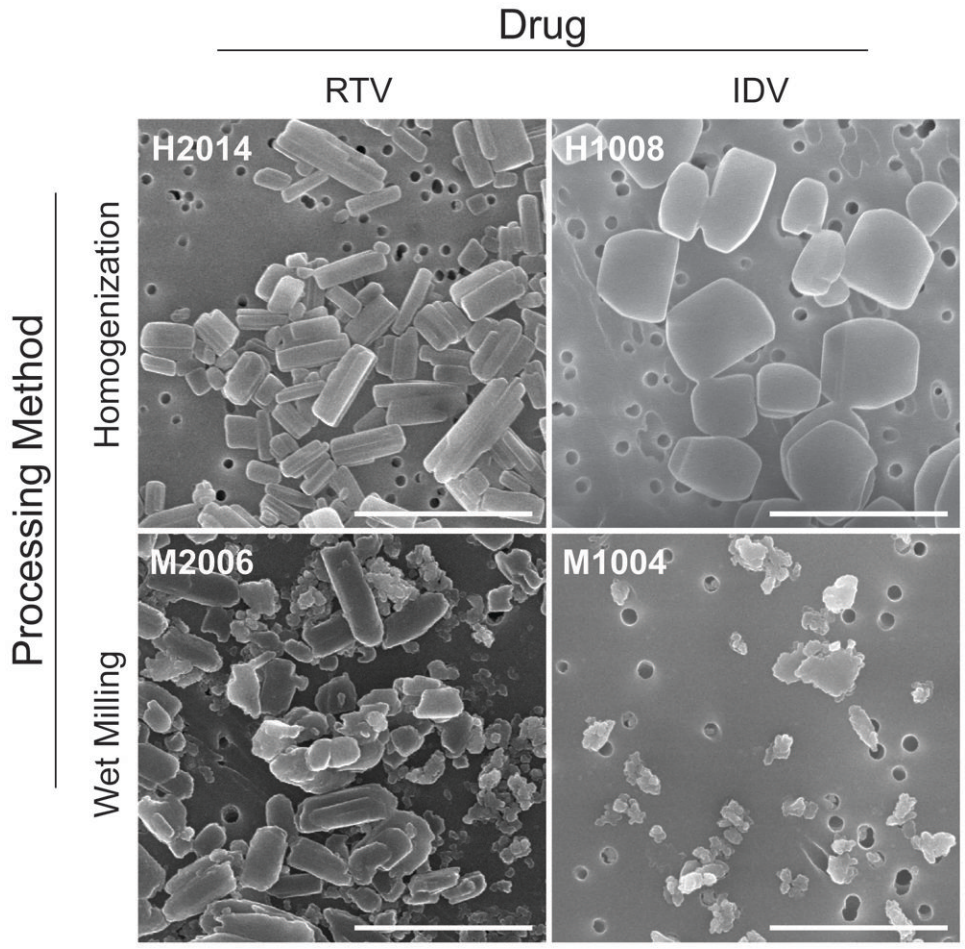

Figure 1. NanoART morphology

Scanning electron microscopy analysis (magnification, 15,000X) of nanoformulations of RTV (H1023 and M1016) and IDV (H1012 and M1002) on top of a 0.2 μm polycarbonate filtration membrane. IDV NP manufactured by homogenization (H10120) had boulder-like shapes and smooth edges, while those manufactured by wet milling (M1002) were ellipsoid with rough edges. RTV NP manufactured by homogenization (H1023) had short rod shapes with smooth edges; while those manufactured by wet milling (M1016) also had short rod shapes, but had rough edges and sharper corners. Measure bar equal 2 μm in all frames.

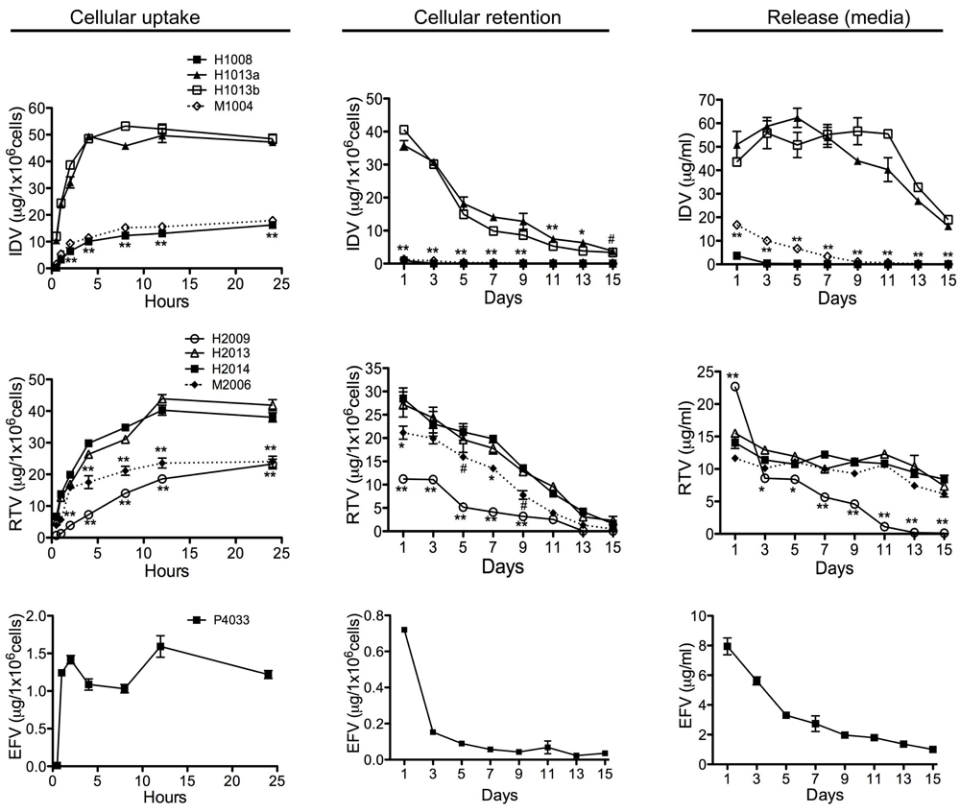

Figure 2. Macrophage uptake, retention and release of nanoformulated IDV, RTV, and EFV

Cellular uptake: MDM were treated with 0.1 mM of each nanoART and levels of H1008, H1013a, H1013b, H2014, H2009, H2013, and EFV in cells quantified by HPLC over 24 hrs. *Cellular retention*: NP-loaded MDM was collected every 2 days over a 15-day period and levels of nanoART in cell lysates quantified by HPLC. *Release*: culture media from NP-loaded MDM was collected every 2 days over a 15-day period and levels of nanoART release quantified by HPLC. ($^{\#}$P<0.05, *P<0.01; **P<0.001).

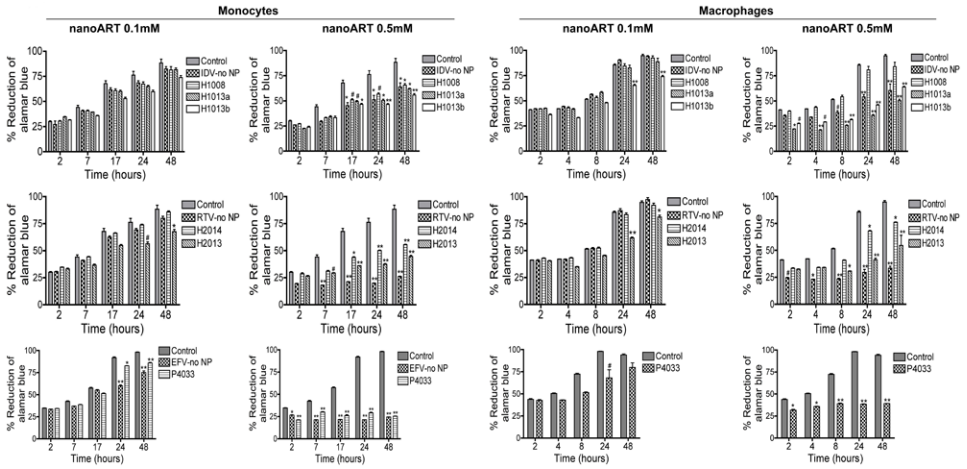

Figure 3. Cytotoxicity profiles for monocyte and MDM nanoART carriage

Monocytes and MDM were loaded for 12 hours with three nanoformulations of IDV (H1008, -H1013 and -H1014), two nanoformulations of RTV (H2014 and -H1027), or P4033 at 0.1 mM and 0.5 mM. Controls consisted of untreated cells and cells exposed to similar concentrations of free (without NP) IDV, RTV, or EFV (IDV-no NP, RTV-no NP, EFV-no NP). Following drug loading, toxicity was assessed over 48 hrs by alamarBlue™ assay. NanoART concentrations of 0.1 mM had minimal or no effect on monocyte and MDM viability, while 0.5 mM significantly increased cytotoxicity. At 0.5 mM drug concentration, increased toxicity was observed in cells exposed to free RTV, compared to cells exposed to nanoformulated RTV. At both 0.1 mM and 0.5 mM, increased toxicity was observed in cells exposed to free EFV, compared to cells exposed to nanoformulated EFV. For each experimental condition, n = 3. Figure shown is representative of 4 independent experiments ($^{\#}P<0.05$, $*P<0.01$; $**P<0.001$).

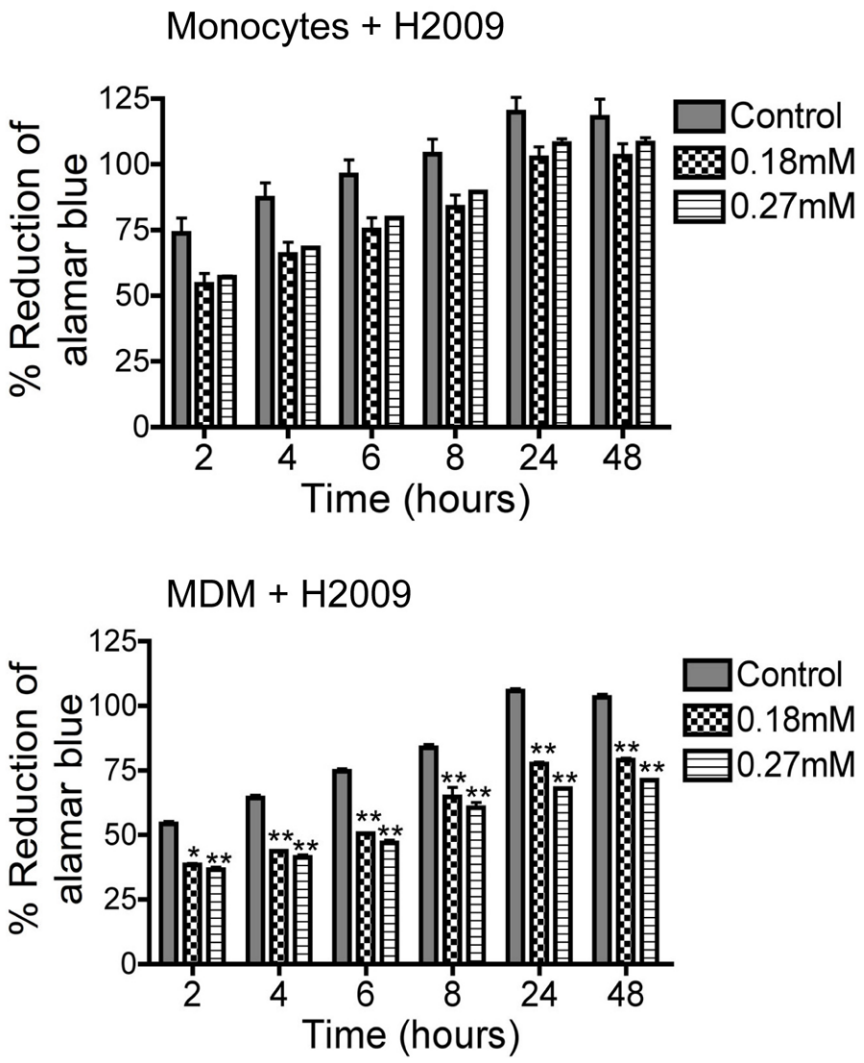

Figure 4. Effects of H2009 on monocyte and MDM viability

Monocytes and MDM were loaded with H2009 at 0.18 and 0.27 mM. Following drug loading, toxicity was assessed over 48 hrs by alamarBlue™ assay. Control consisted of untreated cells. Both H2009 concentrations decreased monocyte viability but the decrease was not statistically significant. Both H2009 concentrations significantly decreased MDM viability (*P<0.01; **P<0.001).

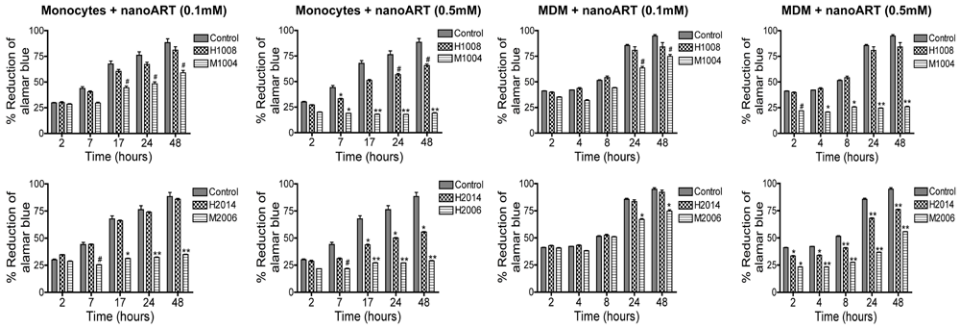

Figure 5. Cytotoxicity of homogenized and wet-milled nanoART on monocytes and MDM

Monocytes and MDM were loaded with homogenized (H1008, H2014) or wet milled (M1002, M2006) formulations at 0.1 mM and 0.5 mM. Following drug loading, toxicity was assessed over 48 hrs by alamarBlue™ assay. Control consisted of untreated cells. Compared to homogenized formulations, wet milled IDV and RTV were significantly more toxic to monocytes and MDM. Comparison of milled nanoART with all homogenized formulations gave similar results. For each experimental condition, n = 3. Figure shown is representative of 3 independent experiments ($^{\#}P<0.05$, $^{*}P<0.01$; $^{**}P<0.001$).

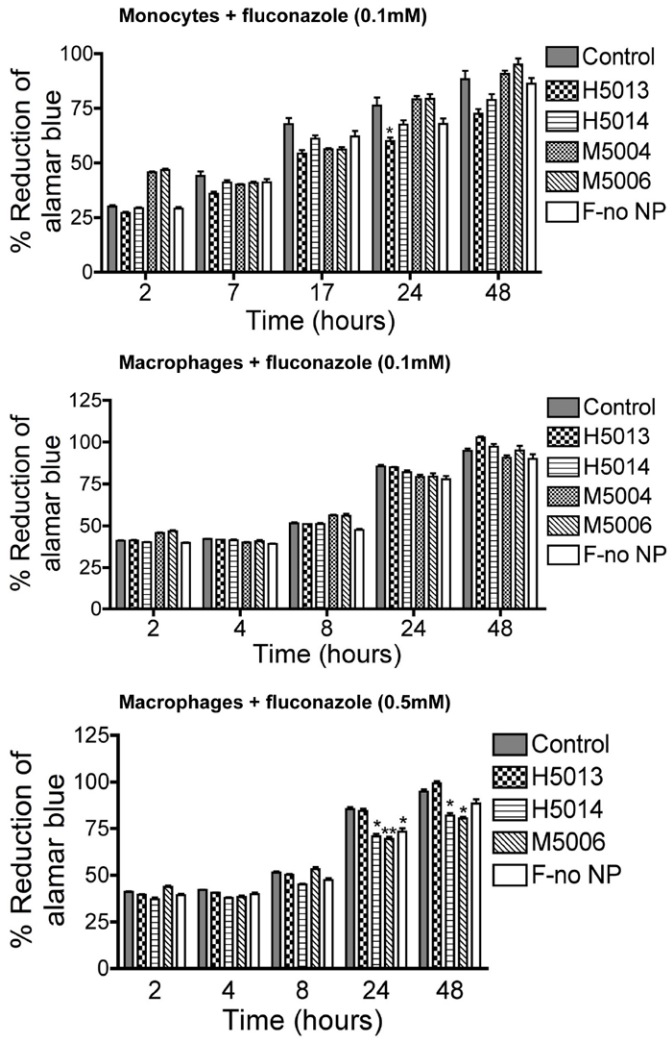

Figure 6. Effect of surfactants and fluconazole on monocyte and MDM viability

Monocytes and MDM were loaded with 0.1 mM or 0.5 mM of individual surfactant or combination of surfactants and fluconazole manufactured using homogenization or wet milling procedures. Additional controls consisted of untreated cells and cells exposed to fluconazole alone (without surfactants, F-no NP). All surfactants and fluconazole controls had no major effect on monocytes or MDM viability. Figure shown is representative of 3 independent experiments (*P<0.01; **P<0.001). Details of surfactant composition are described in Table 1.

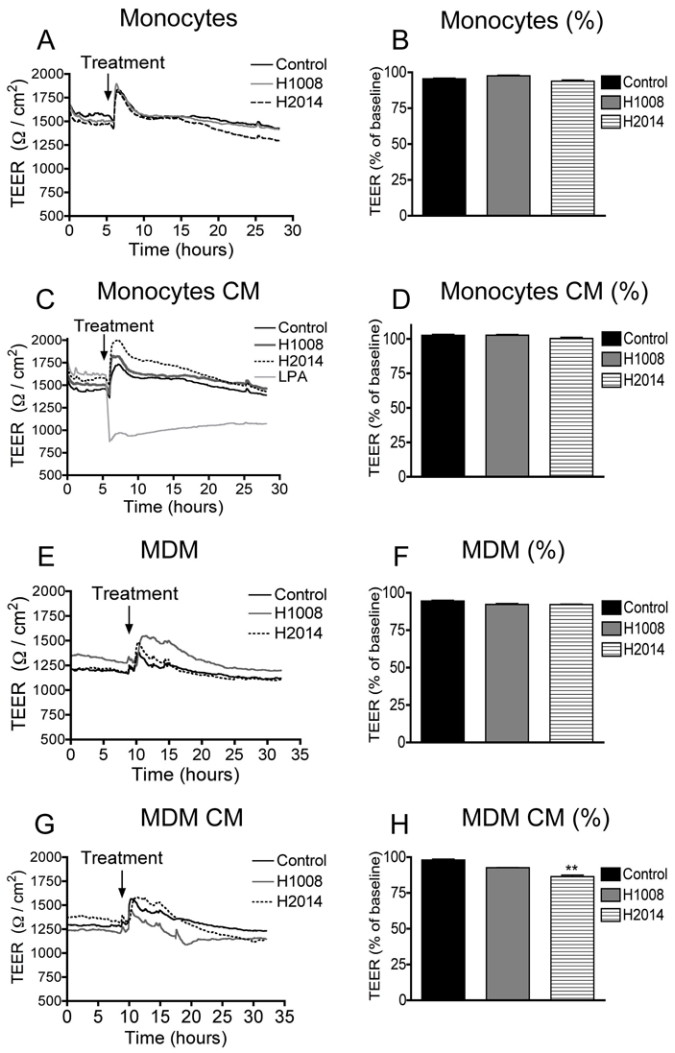

Figure 7. Effect of nanoART on the BBB integrity

Confluent HBMEC were exposed to monocytes (A, B) and MDM (E, F) loaded with H1008 and H2014 (0.5 mM), or exposed to CM from monocytes (C, D) and MDM (G, H) loaded with H1008 and H2014 (0.5 mM), and TEER measured in real-time as described in the Method section. Monocytes or CM from monocytes carrying H1008 and H2014 did not alter TEER (A-D). MDM carrying H1008 or H2014 did not alter TEER (E, F). CM from MDM carrying H1008 reduced the TEER by 5% and CM from MDM-loaded with H2014 decreased TEER by 12% (**P<0.01). Similar results were observed with other nanoformulations and lower concentrations (0.1 mM) did not alter TEER. Data shown are representative of 2 independent experiments. Lysophosphatidic acid was used as a positive control for lowering TEER.

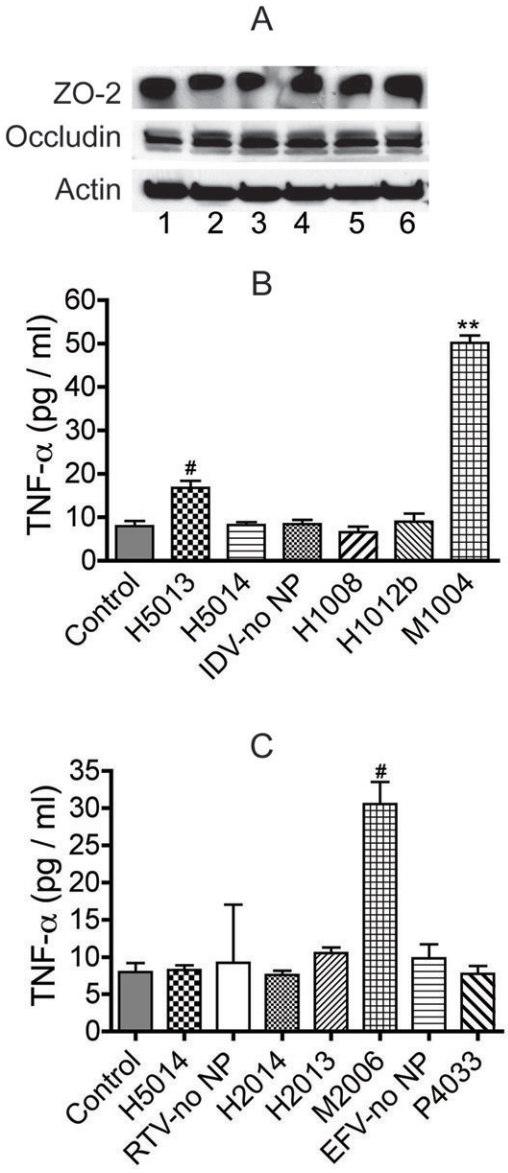

Figure 8. Effect of nanoART on tight junction proteins and TNF-α expression

(**A**) Exposure of HBMEC to monocytes carrying nanoART did not alter expression of ZO-2 and occludin in HBMEC. **1**: control HBMEC (not treated with nanoformulations); **2**: HBMEC exposed to control monocytes; **3, 4, 5, 6** are HBMEC exposed to monocytes loaded with H1008, H2014, H1013b and H2013 respectively. All nanoART were at 0.1 mM concentration. M1002 (**B**) and M2006 (**C**) increased monocytes TNF-α expression ($^{\#}P<0.05$, $^{**}P<0.001$), while all other nanoART did not induce TNF-α expression when compared to controls. Data shown are representative of 3 independent experiments.

Table 1

Physical characteristics of drug nanoparticles

Drug	Formulation	Method	Surfactant	Size (nm)	Zeta Potential (mV)
IDV	H1008	Homogenized	P188, Tween 80	1600	-29.5
	H1013a	Homogenized	P188, $mPEG_{2000}$-DSPE	861	-21.8
	H1013b	Homogenized	P188, $mPEG_{2000}$-DSPE	819	-23.6
	M1002	Milled	P188, SDS	418	-18.73
RTV	H2014	Homogenized	$mPEG_{2000}$-DSPE	500	-26.2
	H2009	Homogenized	$mPEG_{2000}$-DSPE	204	-21.1
	H2013	Homogenized	P188, $mPEG_{2000}$-DSPE	613	-26.7
	M2006	Milled	P188, $mPEG_{2000}$-DSPE	443	-25.93
EFV	P4033	Sonication	PLGA, PVA, CTAB	300	+7.4
Fluconazole	H5013	Homogenized	P188. $mPEG_{2000}$-DSPE	1143	-25.27
	H5014	Homogenized	$mPEG_{2000}$-DSPE	914	-27.36
	M5004	Milled	P188, SDS	530	-20.47
	M5006	Milled	P188, $mPEG_{2000}$-DSPE	894	-26.52

Nanotoxicology. Author manuscript; available in PMC 2013 July 18.